Journal of Structural Geology, Vol. 6, No. 1/2, pp. 159 to 165, 1984
Printed in Great Britain

0191-8141/84 $03.00+0.00
Pergamon Press Ltd.

Secondary lineation in a high-T quartzite (Galicia, Spain): an explanation for an abnormal fabric

J. L. Bouchez, D. H. Mainprice*

Université de Nantes, Laboratoire de Tectonophysique, Chemin de la Houssinière, 44072 Nantes, France

L. Trepied and J. C. Doukhan

Université de Lille, Laboratoire de Structure de l'état solide, Bat. P5., BP 36. 59650 Villeneuve, France

(*Accepted in revised form* 29 *June* 1983)

Abstract—Using refractory inclusions in quartz grains as a marker for the X finite direction (Xf) of the strain undergone by the quartzites it is shown, in our case, that the shape preferred orientation of the quartz grains (Xq), is perpendicular to Xf within the foliation plane and is a secondary lineation. According to that reinterpreted frame, the lattice preferred orientation patterns become 'normal', resulting from the dominant activity of the {m} ⟨*a*⟩ slip systems in a non-coaxial shear regime, and not from [*c*] slip. Development of Xq is attributed to grain-growth during a post-tectonic thermal event, with a faster rate of boundary migration parallel to [*c*] and without substantial change in the lattice fabric. TEM data give support to the latter interpretation but do not demonstrate the absence of [*c*] slip.

This example suggests that a close examination of the significance of the grain-shape lineations is necessary in case of high-temperature deformations. Operation of [*c*] as a dominant slip direction, identified in experimental deformation of high water-content synthetic quartz crystals, is still to be established in natural quartz tectonites.

INTRODUCTION

An impressive amount of work has been done, particularly during the last ten years, concerning the lattice preferred orientations (LPO) of quartz tectonites. Such a renewed interest for fabric studies largely results from the discovery of LPO potential in kinematic analyses of plastically deformed geological bodies, as first applied in peridotites and quartzites (Nicolas *et al.* 1971, 1972, Bouchez 1977a). Also critical for the interest of natural fabrics was the onset of fabric simulation by computer modelling (Etchecopar 1977, Lister 1979, Lister & Paterson 1979) with a view to a better understanding of both the mechanisms of fabric development (slip systems) and the geometrical conditions of the deformation.

An examination of the literature on *c*-axis patterns in natural quartz tectonites reveals that the [*c*] axes are mostly disposed at a high angle to the stretching lineation (X finite). Experimental evidence (Christie *et al.* 1964) as well as detailed studies of grain-shape vs LPO at low temperature (Bouchez 1977b), and considerations on the respective positions of [*c*] and ⟨*a*⟩ with respect to the structural frame (Wilson 1975, Bouchez 1978) have progressively accredited the idea that the dominant slip direction in natural quartz rocks for various (T, σ) conditions is ⟨*a*⟩; the slip planes are in a zone around ⟨*a*⟩, with dominant (0001) at low temperature and $\{10\bar{1}0\}$ and/or presumably $\{10\bar{1}1\}$ at higher temperatures (Bouchez & Pêcher 1981). However, the prism-[*c*] slip systems have been demonstrated to operate in high water-content synthetic crystals (Blacic 1975, Kirby & McCormick 1979). Along with basal-⟨*a*⟩, operation of prism-[*c*] has been suggested by Lister & Dornsiepen (1982) to be responsible for the large opening angle of the *c*-axis crossed-girdle patterns on the Saxony granulites, but no case has been reported which can be interpreted as due to the dominant [*c*]-slip direction, except the case which is presently under study.

Here reported and discussed is the case of a quartzite which displays a strong *c*-axis maximum parallel to the 'quartz lineation'. This case, considered as an unusual fabric, raises the question of the possibility of dominant [*c*]-slip in natural quartzites. We give here optical and TEM arguments tending to demonstrate that the 'quartz lineation' referred to above is a secondary lineation which appeared later in the tectonic history of the rock.

PREVIOUS WORK

The quartz tectonite under study belongs to the 'Armorican' quartzites (Ordovician) of the Galician virgation (Northern Spain). It was collected by P. Matte (1968; GAE 9 oriented sample) in the Sierra de Caurel about 10 km south-southeast of the locality of Sarria, along the inverted limb of a huge recumbent fold which is illustrated by a cross-section in Matte (1968, fig. 12). The paragenetic environment indicates deformation conditions in the upper amphibolite facies. The foliation of the rock ($\perp Z$), subhorizontal in the field, is clearly defined by the flattened quartz grains, parallel to the preferred planar orientation of white micas in a minor

* Present adress: Department of Metallurgy, University of Oxford, Oxford OX1 3PH, U.K.

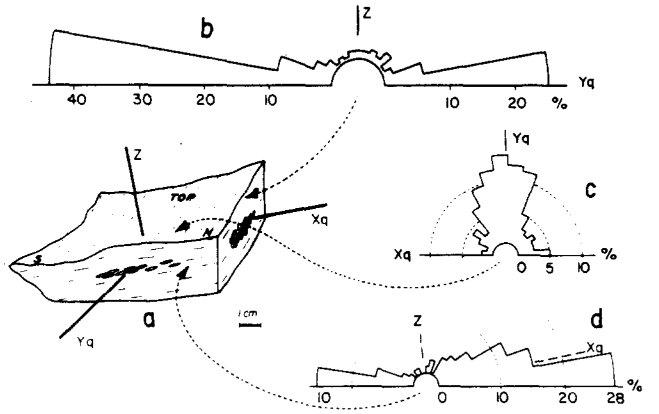

Fig. 1. Sketch of the sample (a) and frequency rose diagrams (b–d) showing the preferred orientation of the elongation directions of the inclusions. (a) The elongate quartz grains are macroscopically visible parallel to the XqZ section; subcircular sections parallel to the YqZ plane. The dashed lines subperpendicular to N–S on the upper surface, parallel a faint mica alignment. The top and bottom boundaries of the sample, locally richer in phyllites, define the macroscopic bedding plane which makes an angle of *c.* 10° with the foliation; this explains the obliquity of Xq with respect to the reference line in (d). (b) YqZ section: almost all the inclusions make a low angle with the section and are elongate close to the Yq direction. (c) $XqYq$ section: 65% of the elongation directions are within Yq + 30°. (d) XqZ section: 52% of the prisms are perpendicular or at a high angle to the section and have not been taken into account; among the remaining 48%, 70% of them are within Xq + 20°.

amount. Within the foliation plane a well-marked grain-shape lineation Xq is defined by the elongation of the quartz grains (Figs. 1a and 3a) trending approximately N–S. In addition to this 'quartz-lineation' a faint 'mica-lineation' trends approximately N 100°E. It appears locally on widely spaced planes of a natural cleavage, corresponding to bands subparallel to the foliation and richer in phyllite. The mica lineation geometrically appears as an intersection line due to the bedding–foliation intersection. This bedding plane, only visible at the outcrop scale, makes an angle of *c.* 10° with the foliation plane in a clockwise sense in reference to the sketch of Fig. 1(a).

The LPO of this rock has been studied by an X-ray goniometry technique (Schmid *et al.* 1981): it is highly pronounced with the [*c*] axes clustering around Xq (Fig. 2b) and the ⟨*a*⟩ axes distributing into three distinct submaxima (Fig. 2c). For the purpose of this paper the preferred orientation of the [*c*] axes has been worked out by optical means (U-stage); as shown in Fig. 2(a), it closely resembles the one derived from the O.D.F. calculation (Fig. 2b). If it is accepted that the LPO results from crystal plastic flow and provided that the quartz-lineation Xq can be equated with X finite, such a distribution of [*c*] and ⟨*a*⟩ with respect to the structural frame ($XqYqZ$) suggests that the dominantly active slip systems were {*a*} [*c*] (Schmid *et al.* 1981).

OPTICAL DATA

A detailed optical microscopy examination reveals that the refractory inclusions within the quartz grains, mainly elongate prisms of zircon (Fig. 3c) and needle-shaped rutile (Fig. 3d), are disposed parallel to the foliation plane and have their average elongation direction perpendicular to Xq (Fig. 1 and caption). The possibility of a crystallographically controlled post-tectonic growth of these inclusions is ruled out for the following reasons. (1) There are fluctuations in alignment of these inclusions within a single quartz grain. (2) Some trails of inclusions have curvilinear trends (Fig. 3e) about their average elongation direction. (3) Some inclusions cross-cut the grain-boundaries (Fig. 3d).

Further optical observations using dark-field illumination, which better outlines the fluid inclusion distribution (Schmid *et al.* 1980, p. 261), strongly suggest the existence of an ancient network of grain-boundaries which does not fit with the present one and which was composed of much smaller cells (~200 μm, Fig. 3g). This network, defined by minute bubbles, is clearly distinct from later linear bubble trails which cross-cut the whole microstructure (Fig. 3h).

TRANSMISSION ELECTRON MICROSCOPY DATA

Thin sections cut from the $XqYq$ and XqZ planes of the specimen have been ion-milled and examined at

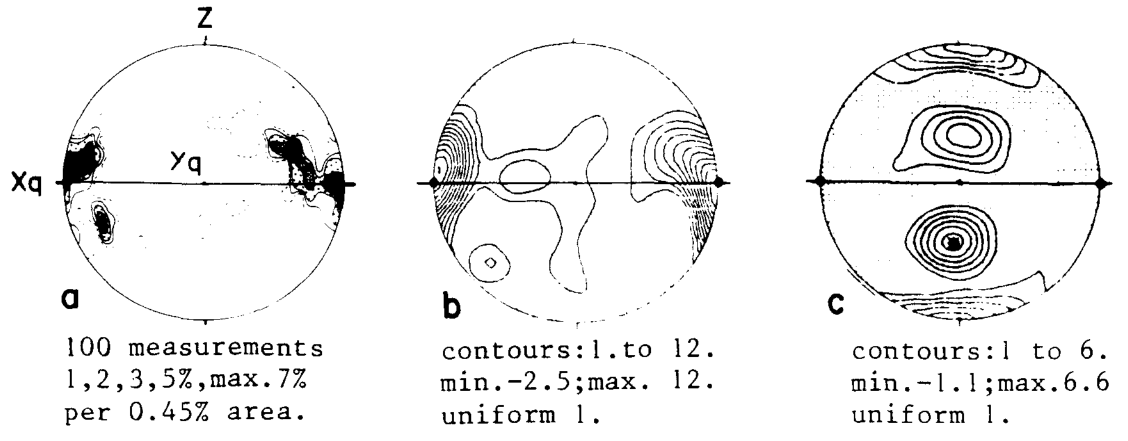

Fig. 2. Lattice preferred orientation diagrams of the Galician quartzite. Equal-area projections. Solid line: rock foliation (⊥ to Z). Xq: quartz lineation = preferred elongation direction of the quartz grains within the foliation plane. (a) *c* axes: U-stage measurements. (b) *c* axes calculated from the O.D.F. (from Schmid *et al.* 1981). (c) ⟨*a*⟩ axes regenerated from the O.D.F. (from Schmid *et al.* 1981).

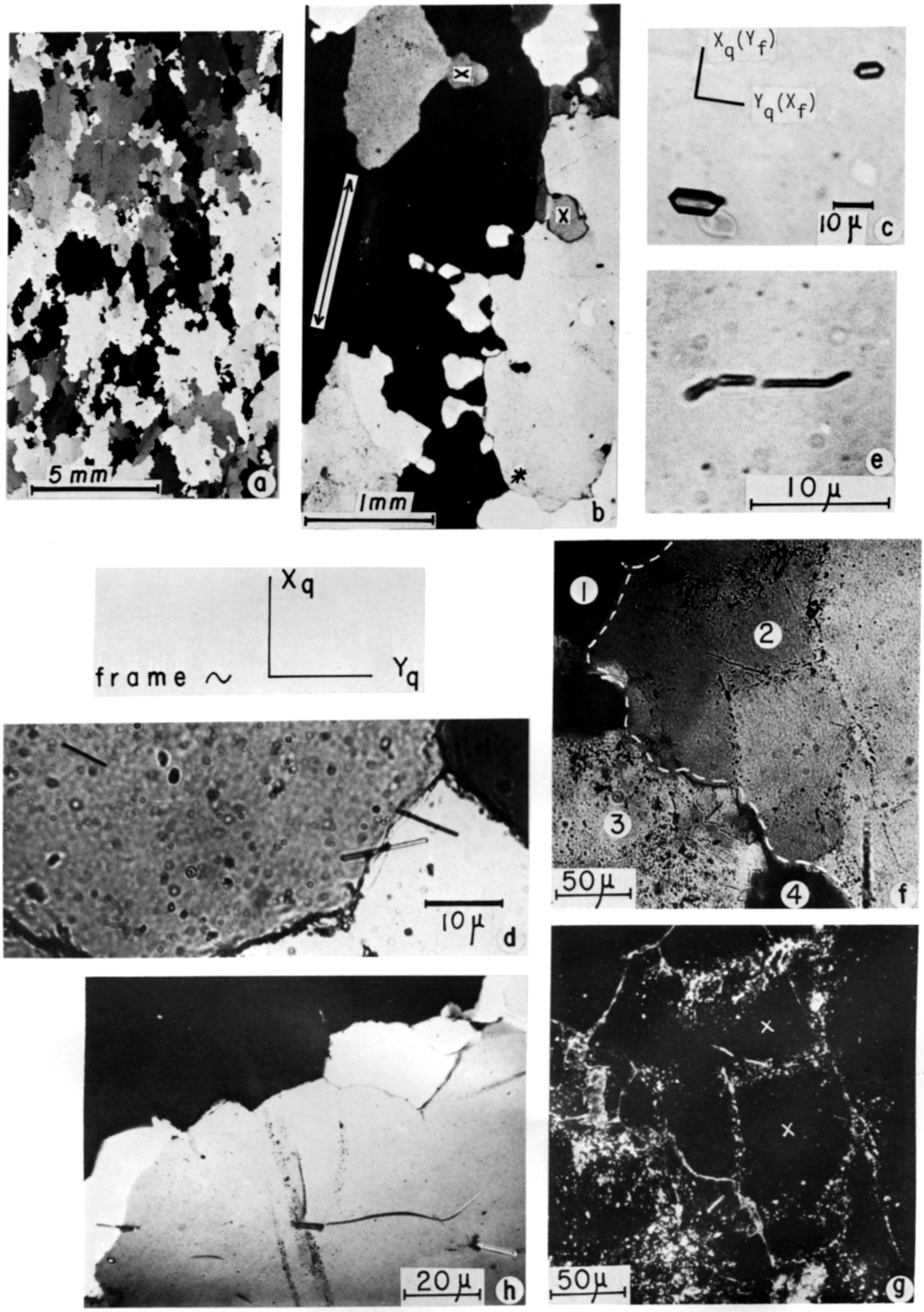

Fig. 3. Optical microstructures of the Galician quartzite. All the photograph planes are parallel to the foliation plane ($XqYq = \perp Z$ plane), with Xq parallel to N–S, and Yq to E–W of the plate (sketched frame). (a) The aggregate; crossed-nicols. (b) Grain boundary bulging (cross) indicative of migration; arrow: possible fastest direction of migration, parallel to Xq; note the optically visible sub-boundaries (parallel to Xq) and the tendency to equilibrated triple junctions (star); photo from Schmid *et al.* (1981, p. 104). (c) Prisms of zircon. (d) Needle-shaped inclusions; two of them are cross-cutting a grain boundary; the average elongation direction is Yq. (e) Pulled apart and reoriented pieces of an original single needle. (f) and (g) Normal illumination (f) with polarizer at 45° to analyser and dark-field illumination (g) of the same area showing cells (crosses) outlined by bubbles (old grains?) and their position with respect to the present grains 1, 2 (contour: white broken line), 3 and 4. (h) Cross-cutting linear trail of fluid inclusions.

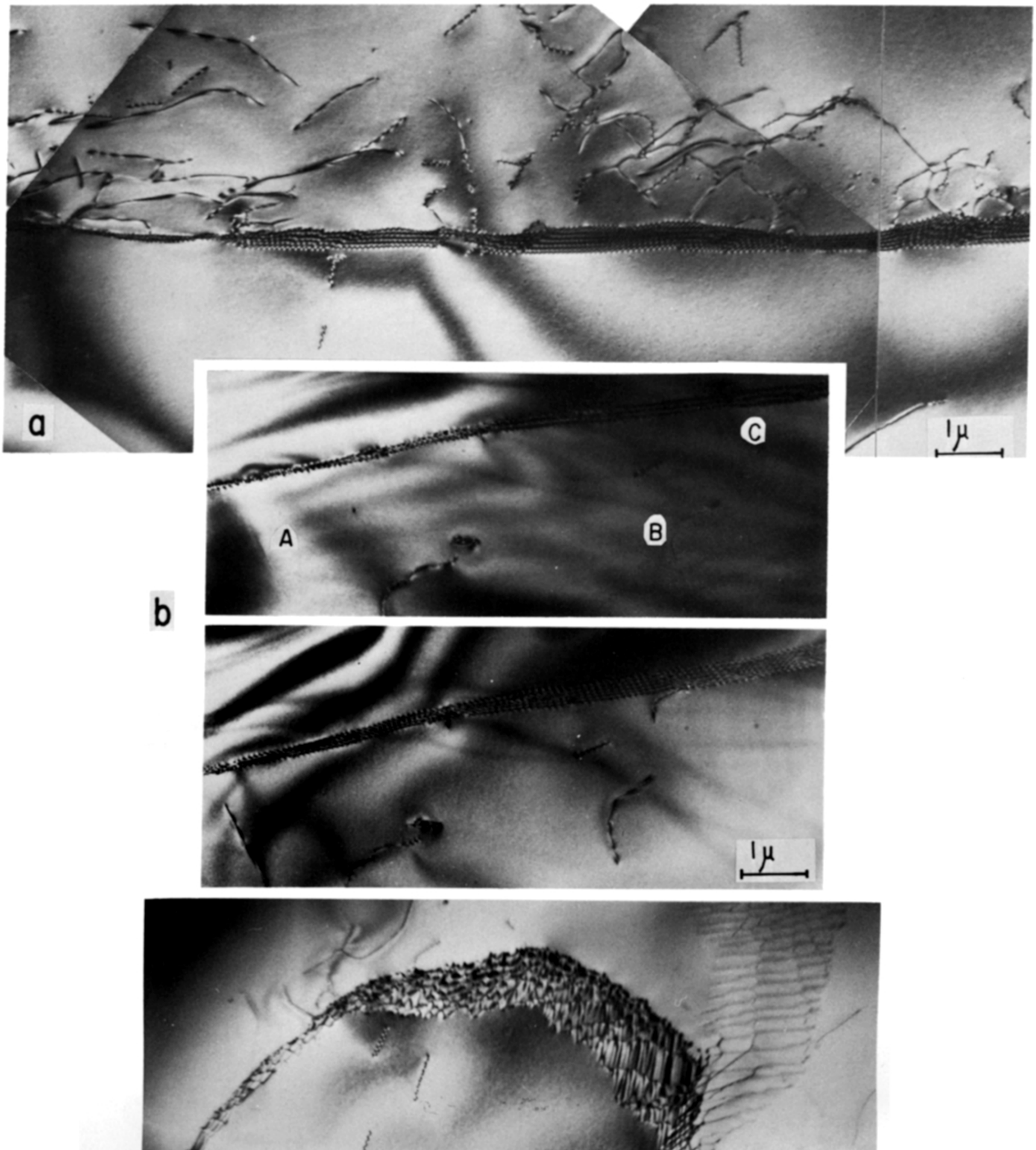

Fig. 4. T.E.M. microstructures of the Galician quartzite. (a) Long and straight twist sub-boundaries (type 1) in the $(10\bar{1}0)$ plane, made of $\langle a \rangle$ and $[c]$ screws; note the rather straight unbound $\langle a \rangle$ dislocations (upper) and the heterogeneity of the distribution (lower). (b) Type 1 sub-boundary (see a); upper: $g = (\bar{1}011)$, dislocations at A, B and C show weak contrast; lower: $g = (\bar{1}101)$, dislocations at A, B and C show strong contrast. The Burgers vector of A, B and C is then $\frac{1}{3}[\bar{1}2\bar{1}0]$ or $[C-a_3]$ (see Trépied & Doukhan 1982). Note the change in direction of the dislocation C (lower) from a 60° dislocation to a pure screw into the sub-boundary. (c) Type 2 curved sub-boundaries intersecting at a triple point. The planes of these boundaries are irrational. Note the long $\langle a \rangle$ direction segments and the short $\langle c+a \rangle$ ones in the sub-boundaries. Straight $\langle a \rangle$ free dislocations in $\{10\bar{1}0\}$.

120 kV in a JEOL-120 CX (Nantes; D.H.M.) and at 100 kV in a Philips EM 300 (Lille; L.T.). The large grain size (~2 mm) allowed individual grains to be selected for detailed crystallographic work.

The microstructure reveals the following two main facts: (1) the density of unbound dislocations is low and (2) the subgrain-boundaries (SGB) are well organized.

(1) The density of free dislocations is heterogeneous at the micron scale (Figs. 4a & c) with a maximum value of $10^7 cm^{-2}$. Most of these dislocations are straight with ⟨*a*⟩ Burgers vectors, lying in {10$\bar{1}$0} and accessorily {10$\bar{1}$1} planes as in Fig. 4(b). Some ⟨*c* + *a*⟩ dislocations are also observed.

(2) The SGBs belong to two groups which are equally represented. Type 1 (Figs. 4a & b) consists of long and straight parallel twist boundaries, 10–20 μm apart. Their habit plane is (10$\bar{1}$0) and the constitutive dislocations are pure screws with $\frac{1}{3}$ [1$\bar{2}$10] and [0001] as Burgers vectors with similar densities. These SGBs are well organized (no long-range stress) but this does not imply that they were formed at high temperature. Indeed, only a minor amount of climb is required for the organization of such SGBs formed by screw dislocations (Trépied *et al.* 1980). Furthermore, segments of unbound dislocations in the edge orientation with an ⟨*a*⟩ or ⟨*c* + *a*⟩ Burgers vector could be traced up to the SGB where they become pure screws (Fig. 4b at site C). Type 2 (Fig. 4c) forms a three-dimensional and irregular array made of scalloped boundaries either irrational or with an approximately rhombohedral {$\bar{1}$101} habit plane. The dislocation density and geometry vary with boundary orientation, being either curvilinear segments sub-parallel to an ⟨*a*⟩ direction with an ⟨*a*⟩ Burgers vector, or segments sub-parallel to ⟨*c* + *a*⟩ directions (Burgers vector not identified).

DISCUSSION

TEM data

Provided that the recrystallization processes remain moderate, it is conceivable that some traces of the deformation undergone by the quartz grains are preserved. In fact, reorganization of free dislocations in SGBs during recovery bears some memory of the slip systems (Trépied *et al.* 1980). Therefore, if [*c*] slip was dominant, one should find dislocations with the [*c*] Burgers vector, either free and confined into their {10$\bar{1}$0} and/or {11$\bar{2}$0} slip planes, or in SGBs mainly made of [*c*] dislocations. Among the observed free dislocations, no one was found with a [*c*] Burgers vector, suggesting either that they never existed or that they have been erased. In the latter case the presently visible dislocations could represent a late strain event. But the close relationship of some of them with Type 1 SGBs makes it unlikely (Fig. 4b). The geometry of Type 1 sub-boundaries fits with an origin by slip and recovery. They do contain [*c*] dislocations, but knowing of experimental situations where secondary slip systems are activated during annealing, allowing the relaxation of the SGBs (Crampon *et al.* 1974), the actual [*c*] could be generated in localized places in order to relax the stress fields due to the previously activated ⟨*a*⟩ slip systems. The observation of free ⟨*a*⟩ dislocations joining the sub-boundary (Fig. 4b) supports this view. Hence, the data relative to Type 1 SGBs much more document the activity of ⟨*a*⟩ slip than that of [*c*]. The Type 2 sub-boundaries, although well organized with no long range internal stress, have a geometry which does not fit with an origin by recovery of slip dislocations. Rather they are to be associated with a recrystallization process (climb).

The heterogeneous and low dislocation density as well as the wavy Type 2 sub-boundaries are in favour of a recrystallization episode post-dating the main deformation event. It cannot be argued whether Type 1 SGBs are relict microstructures (prior to grain-growth) or new ones. The latter is plausible considering the optically visible (prismatic) sub-boundaries (Fig. 3b), resulting from ⟨*a*⟩-slip, and which probably appeared during a late low-T strain pulse.

In short, the TEM data give no evidence for [*c*]-slip. If [*c*]-slip was active at one time, its microstructural signature has been erased.

Xq *is at right angle to* X *finite*

We consider that the elongate solid inclusions have been reoriented towards the stretching direction by crystal plastic flow; accordingly the average elongation direction of the whole population of inclusions, approximately parallel to *Yq* (Fig. 1c), should be equated to *X* finite. The existence of such a reorienting phenomenon of solid inclusions within deforming quartz has been demonstrated and used as a strain marker by Mitra (1976) in low-T porphyroclastic quartzites. Reoriented and stretched inclusions are now frequently used as a microstructural tool in quartz-rich tectonites (Freeman 1982, Diot *et al.* 1983). The main difference with the latter authors' observations is that, here, pulled-apart needles are scarce and the amount of stretching is far less intense in our rock (Fig. 3e). This could be due to a higher viscosity contrast between quartz and refractories in this high-T deformed rock.

When placed in a geographical frame, the *X* finite direction remains subhorizontal and trends approximately E–W, more or less parallel to the axes of the megascopic folds in the area. It is also parallel to the direction of the boudinage structures described in the Sierra de Caurel (Matte 1968, fig. 75) and to the stretching lineations which have been mapped slightly to the north along the Galician virgation (Matte 1968, fig. 44).

A secondary thermal event is responsible for Xq

The regional petrological descriptions of Capdevilla (1967) and Matte (1968) indicate that the major tectonic phase (horizontal foliation and recumbent folding) took

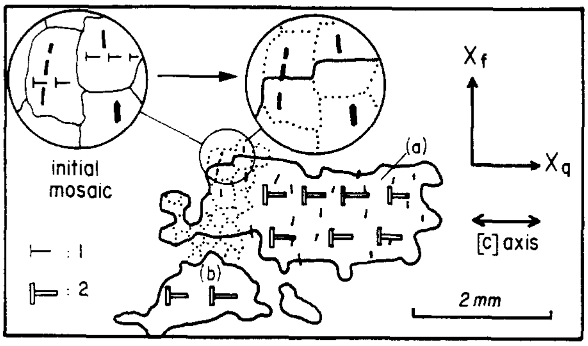

Fig. 5. Proposed microstructural evolution. Section parallel to the foliation plane. Refractory inclusions aligned sub-parallel to *Xf*. Initial mosaic: the sub-boundaries (1) are prismatic, normal to *Xf*. The annealed microstructure now observed has large grains with a complicated geometry in three dimensions. The grain sectioned at (a) is the same grain observed at (b): this geometry is typical of high temperature grain growth (see Schmid *et al.* 1980). Old grain boundaries are marked by the stippled lines, and the new, prismatic, sub-boundaries (2) are disposed parallel to the grain elongation *Xq* (see Fig. 3b).

place under mesozonal conditions, predating the thermal peak which attains the sillimanite grade (Matte 1968, fig. 124). This fits with our TEM data (see above). At the optical scale, the large size of the quartz grains (up to 2 mm), much larger than the presumed ancient ones (Fig. 3g), and the frequent bulging of the grain-boundaries (Fig. 3b) point to grain growth. In addition, grain-boundary mobility has been operating at least partly after the main deformation episode, that is after the inclusions have been reoriented. This is supported by fluctuations in the inclusion alignment within the same grain, pointing to an origin from different initial grains, and by observations of inclusions crossing over grain boundaries (Fig. 3d).

The mechanism by which the new lineation *Xq* develops out of the initial aggregate is not that clear. As *Xq* is parallel to the maximum of the [*c*] axes, it is suggested that the boundaries were migrating faster parallel to the [*c*] axis of quartz, perhaps channelled by the original sub-boundaries which appeared parallel to [*c*] during the crystal plastic flow (normal to the ⟨*a*⟩-slip direction (Fig. 5)). It is noteworthy here that a somewhat comparable situation leading to a secondary foliation has been described in peridotites by Coisy (1977, p. 20). In his case, the new grain boundaries were shown to derive from the progessive misorientation of the (100) tilt sub-boundaries during plastic strain, but the boundary migration was moderate with as a result a grain-size smaller than the original one.

{*m*} ⟨a⟩ *is the dominant slip system*

If the diagrams of Fig. 2 are now considered according to the finite strain framework, where *Xq* is replaced by *Y* finite and *Yq* by *X* finite, the fabric of the quartzite is not unusual and suggests the dominant activity of the {m} ⟨*a*⟩-slip system. Such a '*Y* maximum' fabric for the [*c*] axes has been encountered among others in quartz-ribbon mylonites (Wilson 1975) and in the Angers ribbon-grains and orthogneiss (Bouchez 1977b). The unequally populated submaxima of the ⟨*a*⟩ axes on each side of *Xf* (submaxima at 4 and 6 in Fig. 2c) point to a non-coaxial shear regime for this Galician tectonite.

CONCLUSIONS

It is proposed that the quartz aggregate we are dealing with was originally rather fine-grained (~200 μm) and was deforming, under upper amphibolite temperature conditions, in such a way that *Xf*, *Yf* and *Z* were the principal axes of the finite strain ellipsoid; *Xf* being parallel to the average elongation direction of the passively reoriented solid inclusions. The deformation regime was essentially non-coaxial, say close to simple shear, in a thrust environment with its regionally flat foliation. As a consequence a strong LPO developed, with a strong concentration of the ⟨*a*⟩ axes at an angle to *X* finite (due both to the non-coaxial shear and the dominant ⟨*a*⟩ slip direction), and a strong '*Y*-maximum' of the [*c*] axes (due to the dominant {m} slip planes). That major deformation episode was followed by a period of annealing which was responsible for grain-growth. A set of strain-induced high-angle prismatic sub-boundaries, hence subnormal to *X* finite, could have formed progressively. During annealing (Capdevilla 1967, Matte 1968) grain growth took place with the migration of the boundaries possibly partly channelled parallel to these sub-boundaries (Fig. 5). Being thus faster parallel to [*c*], grain-boundary migration has contributed to the onset of a new grain elongation more or less perpendicular to *X* finite.

We have to conclude that the LPO has not been substantially altered during the annealing and grain-growth episode. This is compatible with Wilson's (1982) observations of an ice aggregate which showed no change in the *c*-axis distribution during annealing after hot-working (−1°C), contrary to what was observed during annealing after cold-working (−10°C). A strengthening of the LPO could even have occurred (concurrently with an order of magnitude increase in grain size) as demonstrated by Green (1967) in a flint which was experimentally deformed at high temperature and then annealed.

In short we think that prism-[*c*] slip is still to be established in natural quartz tectonites. Does the absence of this water-sensitive slip system indicate that the LPO development and consequently the rheology of quartz is not water sensitive in natural conditions?

Acknowledgements—Arnaud Etchecopar (Montpellier) is kindly thanked for providing the samples and for helpful discussion. Adolphe Nicolas critically revised the manuscript. Financial support was provided by the C.N.R.S. (E.R.A. n°547) and by a Royal Society European Exchange Fellowship at Nantes (D.H.M.).

REFERENCES

Blacic, J. D. 1975. Plastic deformation mechanisms in quartz: the effect of water. *Tectonophysics* **27**, 271–294.

Bouchez, J. L. 1977a. Le quartz et la cinématique des zones ductiles. Thèse, Université de Nantes.

Bouchez, J. L. 1977b. Plastic deformation of quartzites at low temperature in an area of natural strain gradient. *Tectonophysics* **39**, 25–50.
Bouchez, J. L. 1978. Preferred orientation of quartz ⟨a⟩ axes in some tectonites: kinematic inferences. *Tectonophysics* **49**, T25–T30.
Bouchez, J. L. & Pêcher, A. 1981. The Himalayan Main Central Thrust pile and its quartz-rich tectonites in Central Nepal. *Tectonophysics* **78**, 23–50.
Capdevila, R. 1967. Extension du métamorphisme régional hercynien dans le Nord-Ouest de l'Espagne (Galice orientale, Asturies, Leon). *C.r. somm. Séanc. Soc. géol. Fr.* **7**, 277–279.
Christie, J. M., Griggs, D. T. & Carter, N. L. 1964. Experimental evidence of basal slip in quartz. *J. Geol.* **72**, 734–756.
Coisy, P. 1977. Structure et chimisme des péridotites en enclaves dans les basaltes du Massif Central français. Modèles géodynamiques du manteau supérieur. Thèse, Université de Nantes.
Crampon, J., Doukhan, J. C., Escaig, B. & Farvaque, J. L. 1974. The thermally activiated deformation of Tellurium single crystals. *Phys. Stat. Sol.* **24**, 167–180.
Diot, H., Bouchez, J. L. & Blaise, J. 1983. La bande ductile Lanvaux-Les-Ponts-de-Cé entre Redon et Angers. Une composante du cisaillement hercynien du Massif Armoricain (France). *Bull. Soc. géol. Fr.* **25**, 155–167.
Etchecopar, A. 1977. A plane kinematic model of progressive deformation in a polycrystalline aggregate. *Tectonophysics* **39**, 121–139.
Freeman, B. 1982. Quartzite deformation mechanisms and deformation mechanism histories. *Mitt. geol. Inst. ETH Univ. Zürich, N.F.* **269a**, 103–104.
Green, H. W. 1967. Quartz: extreme preferred orientation produced by annealing. *Science, Wash.* **157**, 1444–1447.
Kirby, S. H. & McCormick, J. W. 1979. Creep of hydrolytically weakened synthetic quartz crystals oriented to promote {2110} ⟨0001⟩ slip: a brief summary of work to date. *Bull. Minéral.* **102**, 124–137.
Lister, G. S. 1979. Fabric transitions in plastically deformed quartzites: competition between basal, prism and rhomb systems. *Bull. Minéral.* **102**, 232–241.
Lister, G. S. & Paterson, M. S. 1979. The simulation of fabric development during plastic deformation and its application to quartzites: fabric transitions. *J. Struct. Geol.* **1**, 99–115.
Lister, G. S. & Dornsiepen, U. F. 1982. Fabric transitions in the Saxony granulite terrain. *J. Struct. Geol.* **4**, 81–92.
Matte, P. 1968. La structure de la virgation hercynienne de Galice (Espagne). *Trav. Lab. Géol. Fac. Sci. Grenoble* **44**.
Mitra, S. 1976. A quantitative study of deformation mechanisms and finite strain in quartzites. *Contr. Miner. Petrol.* **59**, 203–226.
Nicolas, A., Bouchez, J. L., Boudier, F. & Mercier, J. C. 1971. Textures, structures and fabrics due to solid state flow in some European lherzolites. *Tectonophysics* **12**, 55–86.
Nicolas, A., Bouchez, J. L. & Boudier, F. 1972. Interprétation cinématique des déformations plastiques dans le massif lherzolitique de Lanzo (Alpes piémontaises). Comparaison avec d'autres massifs. *Tectonophysics* **14**, 143–171.
Schmid, S. M., Paterson, M. S. & Boland, J. N. 1980. High temperature flow and dynamic recrystallization in Carrara marble. *Tectonophysics* **65**, 245–280.
Schmid, S. M., Casey, M. & Starkey, J. 1981. An illustration of the advantages of a complete texture analysis described by the orientation distribution function (O.D.F.) using quartz pole figure data. *Tectonophysics* **78**, 101–117.
Trépied, L., Doukhan, J. C. & Paquet, J. 1980. Subgrain boundaries in quartz: theoretical analysis and microscopic observations. *Phys. Chem. Min.* **5**, 201–218.
Trépied, L. & Doukhan, J. C. 1982. Evidence of ⟨a + c⟩ dislocations in synthetic quartz single crystals compressed along the c-axis. *Bull. Minéral.* **105**, 176–180.
Wilson, C. J. L. 1975. Preferred orientation in quartz ribbon mylonites. *Bull. geol. Soc. Am.* **86**, 968–974.
Wilson, C. J. L. 1982. Texture and grain growth during the annealing of ice. *Textures and Microstructures* **5**, 19–31.